IJCRT.ORG ISSN : 2320-2882

INTERNATIONAL JOURNAL OF CREATIVE RESEARCH THOUGHTS (IJCRT)

An International Open Access, Peer-reviewed, Refereed Journal

Rietveld Refinement, Williamson-Hall Analysis of XRD Data and Frequency Dependent Electrical Studies of Zr^{4+} Doped $PbTiO_3$

Kapil Vaishnave[1] , Rajesh Kumar Katare[2]

[1]Research Scholar, Dept. Of Physics, SAGE University, Indore (M.P.)-India

[2] Professor, Dept. Of Physics, SAGE University, Indore (M.P.)-India

Abstract: Numerous multipurpose perovskite materials have been prepared in recent years as a result of the remarkable versatility of perovskite structure in accommodating various dopant ions. By doping divalent Zr^{4+} ions into the octahedral positions of lead zirconate-titanate perovskite, we hope to create stable and extremely high dielectric constant lead-based materials for supercapacitors. Due to its intriguing ferroelectric, dielectric, piezoelectric, and other electrical properties, lead titanate based materials have attracted a lot of attention from material scientists.Here in this study, we report synthesis of $PbZr_{0.01}Ti_{0.99}O_3$ material by high temperature solid synthesis technique. The Rietveld refinement of the sample confirms the pure phase of tetragonal structure with space group of P4mm.William son-Hall analysis of the XRD data revels the size of crystallite to be about 50nm and the strain arising from the high firing and intense grinding effect to be $8.54*10^{-3}$. The electrical impedance and electrical modulus as a function of ac field was investigated to emphasize on the conduction mechanism in the sample.

Index Terms - **Crystal Structure, Rietveld Refinement, Williamson-Hall Method, Conduction Mechanism**.

I. INTRODUCTION

The intriguing ferroelectric, piezoelectric, and other electrical properties of lead titanate zirconate ($PbZr_{1-x}Ti_xO_3$) commonly denoted as PZT solid solutions have attracted a lot of attention from material scientists. Multilayer capacitors, micro-electromechanical systems (MEMS), and integrated devices including ferroelectric memory, infrared sensors, ic memories, micro actuators, etc are among the many applications for lead-based perovskite ferroelectric ceramics. Materials with superior ferroelectric and dielectric qualities are required for many of these applications. Since the late 1940s, lead zirconium titanate (PZT), one of the best lead-based materials, has been the subject of much research as it shows potential features to fullfill the above requirements

The stoichiometry of PZT ceramic affects its dielectric properties. When PZT compositions are doped with foreign ions, they exhibit notable merit. The site that the foreign ion occupies in the ABO_3 perovskite structure affects its dielectric and piezoelectric characteristics. The attachment of various dopants to the "A" or "B" sites of PZT improves or customizes its features. With the general formula ABO_3 (A = divalent, B = tetravalent cation), PZTs are a member of the perovskite family. Zr^{4+} or Ti^{4+} occupy "B" sites, whereas Pb^{2+} occupies "A" sites. The ability to alter the characteristics of ceramic ferroelectrics by adding dopants that replace a portion of the host atom is one of its many important advantages. A dopant may enter the A site or the B site, depending on its valence and ionic radius. Cation vacancies compensate donor dopants, while oxygen vacancies compensate acceptor dopants.

Solid solutions of lead titanate zirconate ($PbZr_{1-x}Ti_xO_3$), or PZT, crystallize into a variety of deformed perovskite structures. Here, in this report The PZT materials are prepared in bulk by solid state route, investigated for structural, dielectric, morphology, composition and band gap properties. The dielectric properties were studies as a function of frequency and all the characterizations carried out were measured at room temperature

II. EXPERIMENTAL DETAILS

2.1 Sample Synthesis

Using the conventional solid-state reaction ceramic synthesis process, a polycrystalline $PbTi_{0.99}Zr_{0.01}O_3$ sample was prepared. TiO_2, ZrO_2, and PbO were the raw analytic-grade materials. All of these precursors were mixed together in stoichiometric amounts in oxide powder form to form the $PbTi_{0.99}Zr_{0.01}O_3$ sample. The material was mechanically ground for five hours using a pestle and agate mortar. To guarantee that the contents of the sample were dispersed uniformly, acetone was used. calcined in air at 1050 °C for five hours. The same process was repeated at a calcination temperature of 1150 °C.

After the material was calcined, it was crushed for an hour to produce a fine powder that could be used for characterizations. With a pressure of 4 tons per inch, a little amount of the fine powder from the synthesized sample was compressed into pellets with a diameter of 10 mm and a thickness of almost 1 mm. The pellet in the shape of a circular disc was sintered in air at 1200 °C for eight hours. For the purpose of creating an electrode and conducting efficient electrical measurements, the pellet's compact form was polished on its circular faces.

2.2 Characterizations

The crystal structure, phase type, and crystallite size of the $PbTi_{0.99}Zr_{0.01}O_3$ sample was determined using the X-ray powder diffraction technique at room temperature using a Bruker D8-Advance X-ray diffractometer equipped with CuKa1 (1.5406 Å) radiation. The X-ray was generated using 40 kV and 40 mA power settings, and the data was collected with a step size of 0.02° along the angular range 2θ (20° < 2θ < 80°). FullProf refinement software was used to perform Rietveld refinement on the XRD data. Employing UV-Vis spectrometer (Perkin Elmer, Lambda 950 - USA), the sample was examined for optical bandgap by recording the UV-Vis Diffuse Reflectance Spectroscopy (DRS). Using a Novocontrol alpha-A high performance frequency analyzer at room temperature, dielectric measurements were made as a function of frequency in the 100Hz–1MHz range.

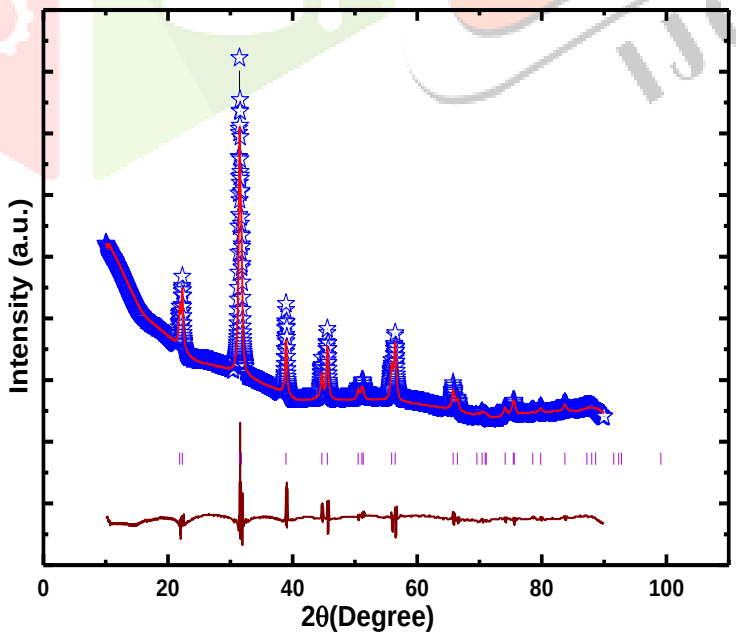

Figure 1: Rietveld Refinement of XRD data of $PbTi_{0.99}Zr_{0.01}O_3$

III. RESULTS AND DISCUSSIONS

3.1 X-ray Diffraction Data Analysis

The X-ray data of $PbTi_{0.99}Zr_{0.01}O_3$ sample was examined for structural analysis using Rietveld refinement. The refined XRD data is displayed as Figure 1. To carry-out Refinement, FullProf software was exploited.

After the complete refinement, it was observed that all the diffraction peaks apparent in the diffraction pattern are matching with the tetragonal phase of the sample. This means that the sample has crystallized into the tetragonal phase and the space group of the phase is P4mm. The accuracy of the phase formation is indicated by the Bragg positions and it is clear that no diffraction peak is left un-refined. After the refinement, various structural parameters were obtained and all the parameters are summarized in the Table 1.

To calculate the particle size and strain induced by mechanical grinding with higher temperature treatment, we used Williamson-Hall method. As W-H approach of particle size determination is an effective method, it has been employed effectively.

Williamson-Hall equation is represented by the equation

$\beta_{hkl} = k\lambda/D\cos\theta + C\varepsilon\tan\theta$ ----------(I)

This equation is re-arranged as

$\beta_{hkl}\cos\theta = k\lambda/D + C\,\varepsilon\sin\theta$ ---------- (II)

Here, β is full width at half maximum and, k = 0.9 is called the shape factor, λ= 1.5406Å is the wavelength of the X-rays used, C is taken as 4 and D indicates the particle size. The data is arranged according to equation (II). A graph is plotted between $\beta_{hkl}\cos\theta$ along y-axis and $4\varepsilon\sin\theta$ along x- axis and displayed as Figure 2. The graph is then linearly fitted, with the intercept of the linear fit representing the strain caused in the sample and the slope of the graph being used to estimate the particle size. The estimated particle size is approximately about 50nm and strain caused in the as synthesized materials is $8.54*10^{-3}$.

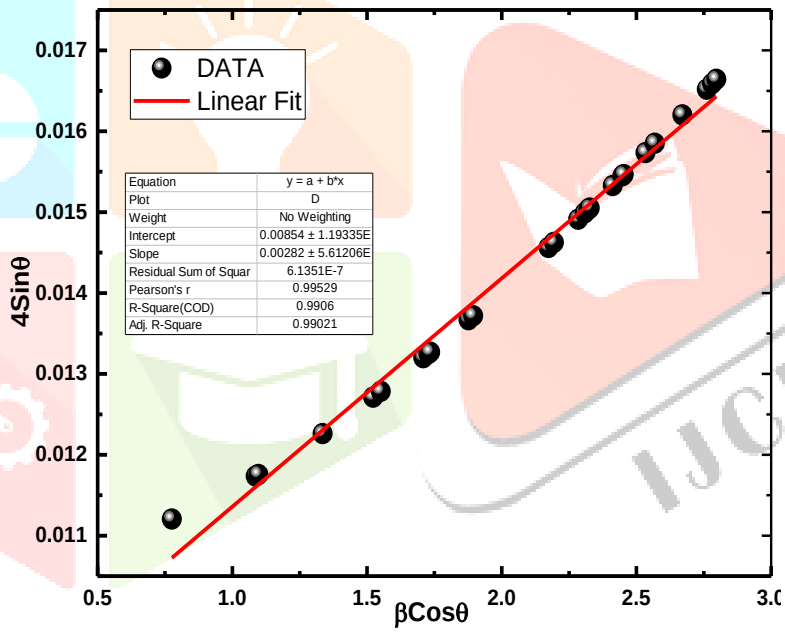

Figure 2: Williamson-Hall analysis for crystallite size determination

Table 1: Structural parameters obtained from Rietveld refinement of XRD data of $PbTi_{0.99}Zr_{0.01}O_3$

Parameters	Numerical Values
Crystal structure	Tetragonal
Space group	P 4/m m m
Lattice parameters	a = 3.9710, b = 3.9710, c = 3.9605 (Å)
Volume	62.4519 $(Å)^3$
density	8.058 g/cm^3
Chi Square (χ^2)	3.2
Goodness of Fit (GoF)	2.4

3.2 Compositional and Micro-structural/Morphological Studies

The $PbTi_{0.99}Zr_{0.01}O_3$sample has been studied for compositional studies using a reliable technique known as energy dispersive analysis of X-rays (EDAX). The EDAX spectrum of the sample is displayed as Figure 3. From the plot, it is evident that all the components of the sample are present. The peaks in the spectrum are intense according to the concentration.

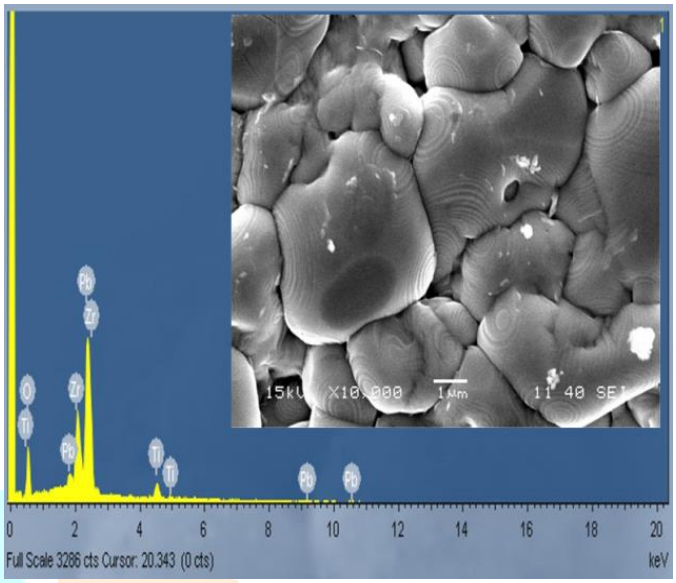

Figure 3: EDX spectrum and FESEM (Inset) image of $PbTi_{0.99}Zr_{0.01}O_3$ sample

The micro-structural studies were carried out using Field emission scanning electron microscopy (FESEM) displayed as inset of Figure 3. It is evident that the grains are well developed and have acquired large size due to diffusion phenomenon facilitated by high temperature treatment. The growth of grains is an agglomeration type process. Furthermore, the grains are well separated from adjacent grains by well-defined grain boundaries. The average grain size is calculated using ImageJ software and the average size of grains is 1.2 micro-meter.

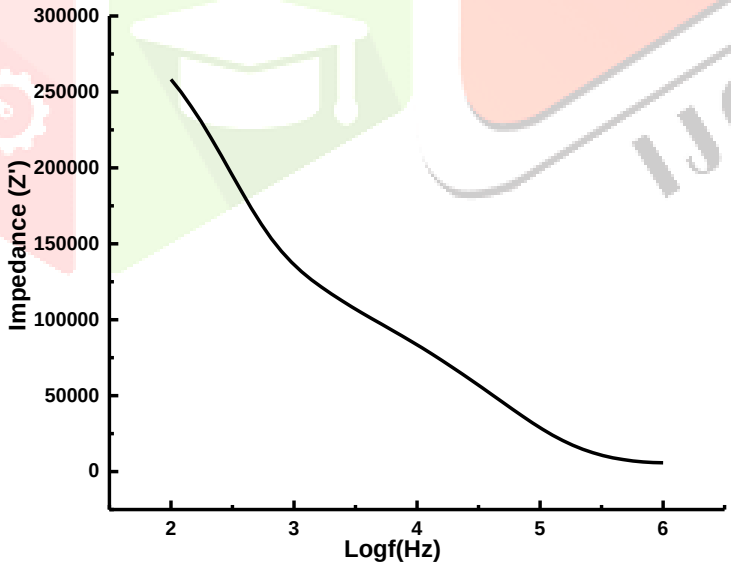

Figure 4: Electrical impedance [Real(Z')] spectrum of $PbTi_{0.99}Zr_{0.01}O_3$ Perovskite sample

3.3 Frequency Dependent Electrical Impedance

The real part of the impedance (Z') varies with frequency, as seen in Figure 4. We observe that when frequency increases, the value of Z' lowers, indicating an increase in ac conductivity. Z' values fall at low frequencies, exhibiting behavior akin to that of semiconductors. The release of space charge brought on by the material's independent at high frequencies. Figure 5 illustrates how the imaginary part of the impedance (-Z") changes with frequency. One broad asymmetric peak is visible; the Z" values rose with frequency, peaked at -Zmax, and then started to decline. This shows how long it takes for a polycrystalline sample to relax.

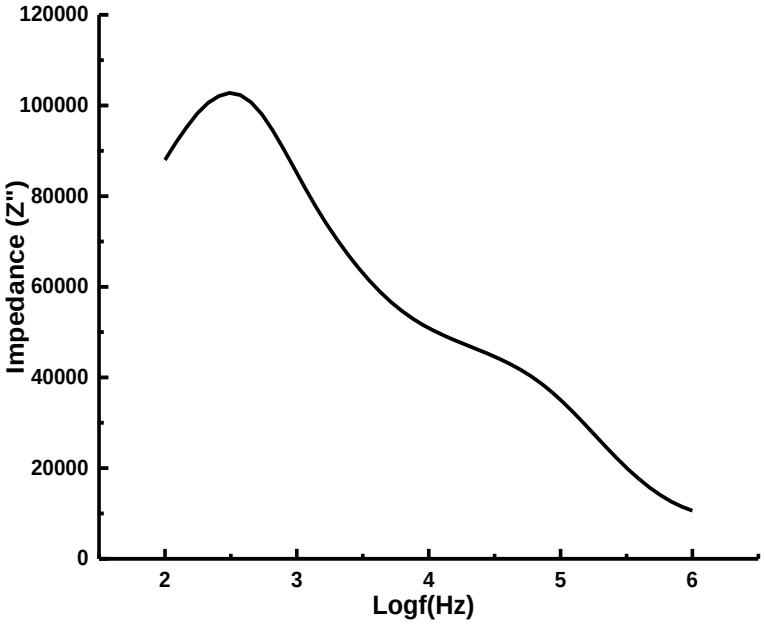

Figure 5: Electrical impedance [Imag(Z″)] spectrum of $PbTi_{0.99}Zr_{0.01}O_3$ Perovskite sample

3.4 Electrical modulus analysis

The electrical modulus formalism is used to study the electrical relaxation mechanism in ion conducting materials. The benefit of this method is that it reduces the impact of electrode polarization. Figure 6 represents real impedance response to applied field and suggests that electrode polarization has minimal impact. Additionally, M' reaches its maximum value at higher frequencies. The dispersion between these frequencies may be due to the relaxation process of conductivity. As frequency rises, a continuous dispersion could be caused by the charge carriers' short-range mobility.

The imaginary component of electric modulus (M") varies with frequency, as shown in Figure 7. The plots in this picture are characterized by the presence of a relaxation peak. The greater frequency of the peak and its asymmetry, which displays the dispersion of relaxation time with different time constants, suggest the non-Debye type of relaxation in the material. The frequency region below the M peak indicates the range in which mobile ions travel over vast distances. In the frequency range above the peak position, the ions have unrestricted mobility within the wells and are spatially limited to prospective wells. The frequency range where the peak occurs suggests a change from long-range to short-range mobility. The relaxation duration of the process was determined using the plot of M vs. Logf (Hz)

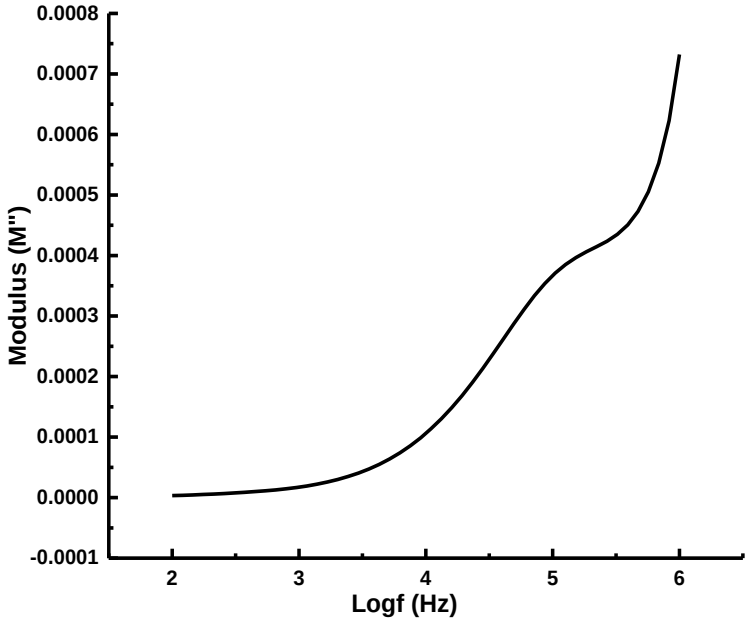

Figure 6: Electrical Modulus [Real(M')] spectrum of $PbTi_{0.99}Zr_{0.01}O_3$ perovskite sample

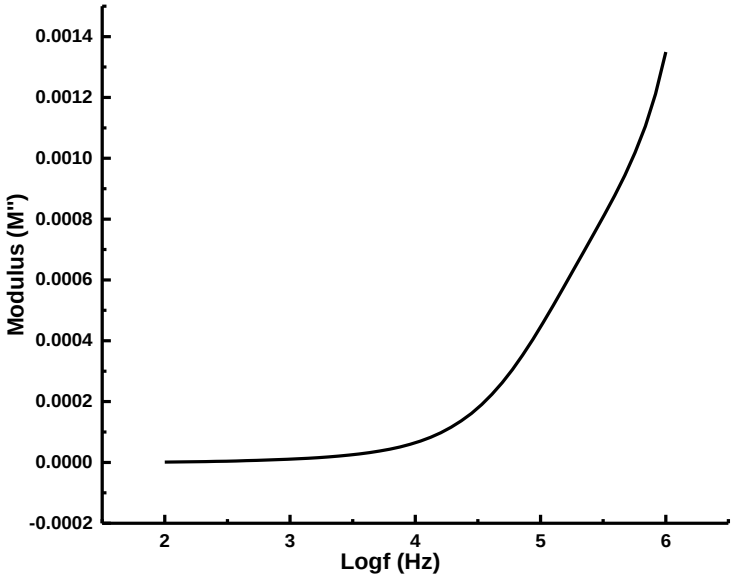

Figure7: Electrical Modulus [Imag(M")] spectrum of $PbTi_{0.99}Zr_{0.01}O_3$ perovskitesample

IV. Conclusion

A polycrystalline $PbTi_{0.99}Zr_{0.01}O_3$ perovskite sample was successfully synthesized by solid state technique. The XRD data fitting by Rietveld refinement method establishes pure phase of tetragonal structure of the sample with space group of P4mm.The tetragonal structured $PbTi_{0.99}Zr_{0.01}O_3$ perovskite sample. Employing Williamson-Hall approach, we estimated particle size to be about 50nm. Compositional study using EDAX technique confirmed the presence of all the constituents of the sample. The FESEM image of the sample reveals that the sample have acquired huge grain size greater than 1micro-meter with well defined grain boundaries separating the grains which is attributed to the diffusion process facilitated by diffusion process arising from intense grinding and high firing effects. The ac field dependent impedance studies reveal the sample behavior akin to the semiconductors whereas electric modulus studies have confirmed dielectric dispersion and non-Debye type relaxations in the sample.

V. Acknowledgment

The authors acknowledge SAGE University as an institute and Department of Physics, SAGE University for providing an opportunity to carry out this research project. Furthermore, the Faculty, labmates and are extended special thanks for cooperation..

References

[1] F. Craciun, E. Dimitriu, B. S. Vasile, C. C. Negrila, R. Trusca, R. Birjega, M. Cernea, The enhancement mechanism of dielectric properties of $Pb(Zr,Ti)O_3$ via (Mg^{2+},Sb^{3+}) incorporation for supercapacitors, Materials Today Chemistry,18 (2020) 100350

[2] L. Wu, S. Kim, C. Moriyoshi, Y. Kuroiwa, M. Suzuki, K. Shinoda, R. Aoyagi and J. Akedo, Synthesis of $Pb(Zr,Ti)O_3$ fine ceramic powder at room temperature by dry mechanochemical solid-state reaction evaluated using synchrotron radiation X-ray diffraction, Jpn. J. Appl. Phys. 60(2021) SFFA02

[3] M. S. Alkathy, Andrews Joseph, K.C. James Raju, Dielectric Properties of Zr substituted Barium Strontium Titanate,Materials Today:Proceedings, 3 (2016) 2321-2328

[4] H. Yang, A. Lyashchenko, X. L. Dong, C. H. Luo, et. al., Fabrication and properties of the Nb doped Zr-rich lead zirconate titanate ceramics by a heterogenous precipitation method, Ceramics International, 33 (2007) 497-503

[5] D. Viehland, Jie-Fang Li, X. Dai, Z. Xu, Structural and property studies of high Zr-content lead zirconate titanate, Journal of Physics and Chemistry of Solids, 57 (1996) 1545-1554

[6] S.S.N Bharadwaja, S Saha, S. Bhattacharyya, S.B Krupanidhi Dielectric properties of La-modified antiferroelectric $PbZrO_3$ thin films, Materials Science and Engineering: B, 88 (2002) 22-25

[7] Z Ujma, L Szymczak, J Hańderek, K Szot, H.J Penkalla Dielectric and pyroelectric properties of Nb-doped $Pb(Zr_{0.92}Ti_{0.08})O_3$ ceramics, Journal of the European Ceramic Society20 (2000) 1003-1010

[8] M. Laurent, U Schreiner, P.A Langjahr, A. E Glazounov, M. .J. Hoffmann Microstructural and electrical characterization of La-doped PZT ceramics prepared by a precursor route, Journal of the European Ceramic Society, 21 (2001) 1495-1498

[9] S. Dutta, R.N.P. Choudhary, P.K. Sinha, Impedance spectroscopy studies on Fe^{3+} ion modified PLZT ceramics, Ceramics International33 (2007) 13-20

[10] R.Ranjan, R. Kumar, B.Behera, R.N.P. Choudhary, Structural and impedance spectroscopic studies of samarium modified lead zirconate titanate ceramics, Physica B: Condensed Matter, 404 (2009) 3709-3716

[11] N. sahu, S. Panigrahi, M. Kar, Structural study of Zr doped $PbTiO_3$ materials by employing Rietveld Method, Advanced Powe technology, 22 (2011) 689-694

[12] V. Mote, Y. Purushotham & B. Dole,Williamson-Hall analysis in estimation of lattice strain in nanometer-sized ZnO particles. J Theor Appl Phys 6 (2012) 6

[13] S. A. A. Jabir, K. H. Harbbi, A comparative study of Williamson-Hall method and size-strain method through X-ray diffraction pattern of cadmium oxide nanoparticle, AIP Conf. Proc. 2307(2020) 020015

[14] M. J. Hoffmann, M.Hammer, A. Endriss , et al. Correlation between microstructure, strain behavior and acoustic emission of soft PZT ceramics. Acta Mater 49:(2001)1301–1310

[15] B. Sahoo, P.K. Panda, Effect of lanthanum, neodymium on piezoelectric, dielectric and ferroelectric properties of PZT Journal of Advanced Ceramics, 2(1) (2013) 37–41

[16] M. A. Mohiudin, A. Kumar, K. L. Yadav, Effect of Nd doping on structural, dielectric and thermodynamic properties of PZT (65/35) ceramics, Physica B, 395 (2007) 1-9

[17] M. R. Soares, A.M.R. Senos, P.Q. Mantas, Phase coexistence and dielectric properties of PZT Ceramic, J. Euro. Ceram. Soc.20 (2000) 321-334

[18] E. Boucher , B. Guiffard, L. Lebrun, D. Guyomar Effects of Zr/Ti ratio on structural, dielectric and piezoelectric properties of Mn- and (Mn, F)-doped lead zirconate titanate ceramics, Ceramics International, 32 (2006) 479-485

[19] B. Tiwari and R. N. P. Choudhary, "Study of impedance parameters of cerium modified lead zirconate titanate ceramics," in IEEE Transactions on Dielectrics and Electrical Insulation, 17 (2010) 5-17.

[20] B.Sahoo , P. K. Panda . Ferroelectric, dielectric and piezoelectric properties of $Pb_{1-x}Ce_x(Zr_{0.60}Ti_{0.40})O_3$, $0 \leq x \leq 0.08$. J Mater Sci, 42 (2007) 9684–9688

[21] V. Kalem, İ. Çam, M. Timuçin, Dielectric and piezoelectric properties of PZT ceramics doped with strontium and lanthanum. Ceram Int , 37 (2011) 1265–1275

[22] A. A. Saif, P. Poopalan, , Effect of the film thickness on the impedance behavior of solgel $Ba_{0.6}Sr_{0.4}TiO_3$ thin films. Physica B. 406 (2011) 1283–1288.